JOURNAL OF AIRCRAFT
Vol. 29, No. 4, July–Aug. 1992

Approach for Analysis and Design of Composite Rotor Blades

Geraldo A. Macedo Moura*
Centro Técnico Aerospacial, São José dos Campos SP, 12225, Brazil
and
Ramesh Kolar†
Naval Postgraduate School, Monterey, California 93943

The developments in tilt rotor technology allow rotor blades to have different twist and rpm requirements in hover and in forward flight to optimize for operational conditions. The available twist of the rotor blade for different flight regimes bears on the performance of the flight. This article presents a detailed analysis of a typical rotor blade, the focus being the static response in the presence of extension-twist coupling induced due to asymmetric stacking sequence of laminas. The baseline rotor blade is modeled as a D-shaped spar using discrete Kirchoff theory-based finite elements. A method is proposed to derive six configurations of blade starting from a base rotor blade made of three laminated shells. The effects of varying rpm and lay-ups for the six configurations are presented as carpet plots in terms of the available tip twist angle. Such plots may be used in the rotor blade design trade-off studies.

Introduction

IN the design of structural components, composite materials offer a wide choice of tailorable stiffness properties. Symmetric laminate constructions may be preferable from an analysis viewpoint by avoiding extension-twist coupling. However, in applications such as tilt rotor aircraft where different flight conditions (hover and forward flight) are encountered, extension-twist coupling of the rotor blade may be used advantageously.[1-3]

This article is directed in using a blade spar to study the sensitivity of the extension-twist coupling due to changes in rpm, layer angle definitions, and changes in laminate orientation.

In the analysis, a program named CASA/GIFTS[4] (Computer Aided Structural Analysis/Graphical Interactive Finite Element Total System) is adopted. Results are reported for six rotor blade models and presented as graphs that show the trends for each model in terms of the available twist.

Rotor Blade Model

Typical rotor system design may be seen as a compromise between the different blade requirements in hover and forward flight, and the mathematical models reflect that tendency or limitation. For instance, the optimum twist for hover is not the same in forward flight for tilt rotors as well as for helicopters. The result is that one of the two flight modes will have less than optimal propulsive efficiency, depending on design phase decisions driven by requirements and/or aircraft mission profiles.

Nixon[2] proposed a model to account for these requirements. The model used an extension-twist coupled rotor blade with 100% rpm (reference value for 100% rpm is 217 rad/s for the rotor blade considered) in hover and 80% rpm in forward flight. These are typical rpms for hover and forward flight for a tilt rotor-type aircraft. The difference in rpm provides a change in centrifugal force, inducing a change in the twist angle distribution, which can be used to optimize the rotor for both flight regimes.

The use of composite materials makes it possible to design a rotor blade that takes advantage of the changing loads, rendering the required twist distribution optimum in each flight mode. At this point a question may be posed: "What is the magnitude of twist available from a particular geometry and material system?"

The answer lies in developing a method of prediction, based on a model that represents the behavior of the blade as accurately as possible. Further, parametric studies to evaluate several geometries and material systems would prove to be fruitful before particular blade designs are selected for manufacture.

The base rotor model analyzed by Hodges et al.[5] was selected for the present study. Results for this rotor model were presented based on MSC/NASTRAN and coupled-beam model.[6] The rotor blade, in this article, was modeled using triangular bending element[7] ("plate/shell element"). Based on discrete Kirchoff theory, the element assumed small displacements and small strains in the formulation and did not include transverse shear and transverse normal strain effects. The element was capable of modeling both symmetric and unsymmetric laminates.[4] The element was validated for laminated composite plates by solving bench mark problems whose analytical solutions were known.

In the present model, the pitching moments generated by aerodynamic loading were not taken into account, the emphasis being on the inertia and extension-twist coupling as sources of torsional moments. An assumed lift distribution acted on the model. The inertia forces acting on the rotating blade produced extension, which caused twist by structural coupling. However, the inertia forces also produced a centrifugal flattening[8] effect called tennis racket effect (because of the tendency of a tennis racket to align its plane with the plane of rotation as it is swung in an arc). This effect may be reduced using balancing weights.

The results comparing the two rotor blade models are presented in Fig. 1. The displacements for the present model appears to be within the assumption of linear, small displacement theory. The models in Fig. 1 have a notation (M120) described in the next section. The discrepancy between the results may be attributed as follows: a possibility that the models compared are not exactly the same, although every effort was made to take into account all the pertinent geometric and material data reported. A twist angle distribution

Presented as Paper 90-1005 at the AIAA/ASME/ASCE/AHS/ASC 31st Structures, Structural Dynamics, and Materials Conference, Long Beach, CA, April 2–4, 1990; received Sept. 22, 1990; revision received March 29, 1991; accepted for publication April 29, 1991.

*Project Manager, Divisão De Aeronáutica.
†Faculty, Department of Aeronautics and Astronautics. Senior Member AIAA.

discrepancy could be explained by the tennis racket effect probably not present in the model described in Ref. 5, but the tip vertical displacement due to lift and weight with no rotation could not be explained by this argument. It may be observed that the displacements quoted in the referenced work are about 25% of the length, which appears to violate the linear theory that was used (detailed comparisons of the two models are being done in a separate study to examine the discrepancies and shall be reported later).

However, this very discrepancy was the motivation and driving force for this article and raises a pertinent question: "What are the possibilities to model different structural configurations starting with the same number of layers, same lay-up design, same thickness and material properties?" (perhaps by inadvertent oversight by designer, or analyst using canned programs, or manufacturing engineer).

In answer to this question, the possibilities of constructing various rotor blade configurations with a given laminate are proposed. This approach of building various rotor blades from the same base laminate provides different stiffness distribution and corresponding response.

In the present modeling process, the following assumptions were made:

1) The structure is a D-shaped spar.

2) It is built using three shells; top, bottom, and rear shell surfaces.

3) The top and bottom meet at the leading edge and the rear shell closes the box.

4) Once established, the internal lay-up in the stacking sequence remains constant.

With these assumptions, a laminate that constitutes one shell surface may be defined, using only the laminate principal orientation (LPO) angle. For example, consider the laminate [+20/−70/+20/−70/−70/+20 deg]. The top layer angle is denoted +20 deg and is a six-layer asymmetric laminate. Rotating the whole laminate 40 deg clockwise gives [−20/+70/−20/+70/+70/−20 deg], and the LPO angle is denoted as −20 deg.

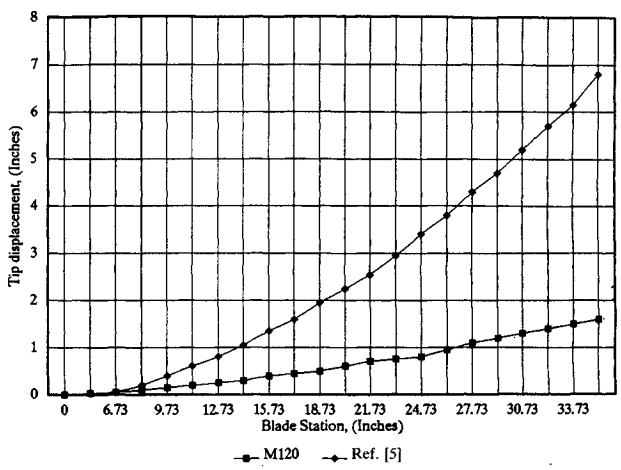

Fig. 1 Tip displacements under lift and weight loads for GIFTS model and Ref. 5.

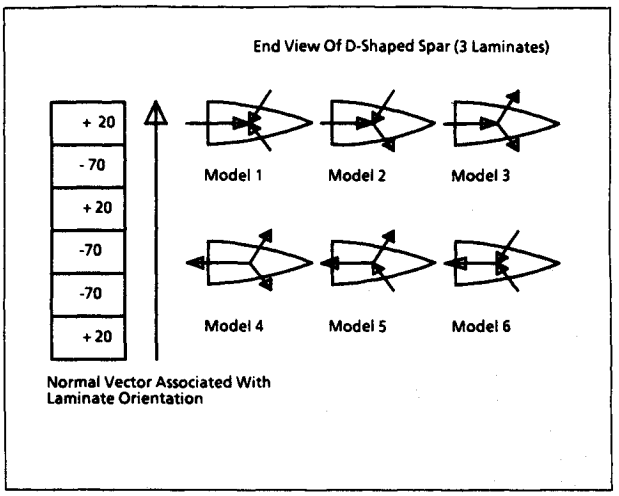

Fig. 2 Normal surface vector associated with the layer sequence of the basic laminate and its position in relation to end view of the blade.

Table 1 Model definitions for six configurations

Models		Surface grid definition		
M1$$	Vector grid def.	L512,L1112,L411,L45[a]	L411,L811,L18,L14[a]	L18,L128,L512,L51[a]
M2$$	Vector grid def.	L512,L1112,L411,L45[a]	L411,L811,L18,L14[a]	L512,L128,L18,L51[b]
M3$$	Vector grid def.	L512,L1112,L411,L45[a]	L18,L811,L411,L14[b]	L512,L128,L18,L51[b]
M4$$	Vector grid def.	L411,L1112,L512,L45[b]	L18,L811,L411,L14[b]	L512,L128,L18,L51[b]
M5$$	Vector grid def.	L411,L1112,L512,L45[b]	L18,L811,L411,L14[b]	L18,L128,L512,L51[a]
M6$$	Vector grid def.	L411,L1112,L512,L45[b]	L411,L811,L18,L14[a]	L18,L128,L512,L51[a]

[a]Vector inward.
[b]Vector outward.

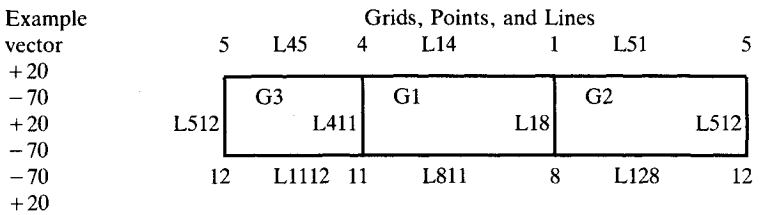

(not to scale, e.g., line L512 is 30.0 in., L45 is 0.286 in., and L14 is about 1.15 in.)

This base laminate has intentionally designed asymmetry to yield extension-twist coupling. Associated with this laminate is a normal vector whose orientation is seen in Fig. 2. The D-spar then is built using three such laminates, with each laminate mounted with the normal vector facing inward or outward. Thus, this method of construction results in six different configurations of the rotor blade. Figure 2 depicts these configurations showing the end view with the arrows pointing the direction of normal vector for each laminate surface. All these illustrations correspond to a LPO of +20 deg. Further, the base laminate (composed of 0/90 deg laminates rotated off-axis) is seen to eliminate hygrothermally induced twist.[2]

The six different configurations are designated M1 through M6 and the LPO angle, which refers to the top layer of the laminate used to construct that particular model, varying from −90 to +90 deg in steps of 20 deg, provides the suffix to complete the model designation as M190 (M190 meaning model 1 with LPO = −90 deg; M340 meaning model 3 with LPO = 40 deg), M340, M660, and so on. There results a total of 11 LPOs in each model (including LPO = 0 deg), with internal stacking sequence essentially remaining the same as defined earlier. Different configurations may be visualized with the help of the scheme shown in Fig. 2. Models 1 and 4 can be built with only one laminate wrapped around, one inverse of the other. In the program GIFTS,[4] the outward vector for each surface is defined during the "GRID" definition; for example, in a four-sided grid, each shell surface is defined when a GRID is specified. The local x axis is oriented parallel to the first line of the grid, the local z axis is the cross product of the first and second "line" in the grid definition, while the local y axis is the cross product of the z and x axes. The outward vector is oriented in a direction defined by the local z axis. Layer angles are positive in the counter-clockwise direction in the xy plane for shell elements, as is the convention for laminated composite materials.

It may be observed that, when an asymmetry is present in the basic laminate (material definition), the structural response is highly dependent on how the grid and consequently the lay-up is defined. In the case of a symmetric laminate or isotropic material, this fact is never brought to surface because of its irrelevancy. However, dealing with asymmetric laminated composite materials, the analyst must always have this in mind.

Table 1 provides a description of various laminate constructions outlined in a compact form. The first column identifies a given model and followed by the grid definition and whether the normal is oriented outward or inward. The line diagram below the table shows the three laminates of a model spread out as three rectangular grids G1, G2, and G3. For each of these models, the rpm, and consequently the centrifugal force, was varied in the range of 130 to 300 rad/s.

The model geometric characteristics are the same as in Hodges et al.,[5] a graphite epoxy composite rotor blade constructed out of Hercules IM6 fiber with Ciba-Geigy R6376 resin. The cured ply thickness is assumed to be 0.0055 in. The D-spar has a 35.23-in. radius, and begins at station 5.23 in., which has all degrees of freedom suppressed to emulate a rigid rotor connection to the hub. The rotor has a constant cross section, defined by 13 nodes and is divided into 21 spanwise (1.5 in. apart) stations. Models with finer meshes were used in the early stages to check for convergence. The mesh selected seemed to be a reasonable compromise between the computational time and accuracy.

The orthotropic material properties of the lamina are listed below:

E_{11}, psi 23.1×10^6

E_{22}, psi 1.4×10^6

ν_{12} 0.338

G_{12}, psi 0.73×10^6

Static Analysis

The six models described were subjected to three main types of independent static loads. A modal analysis was performed to obtain the first four fundamental modes of vibration frequencies and mode shapes as reported in Moura.[9] The first load applied is a torque at the tip, not combined with any other load. The second load case consisted of combined lift and blade weight at zero rpm, i.e., with no centrifugal forces. The third load case was the centrifugal force due to rotation of the blade together with the lift and blade weight.

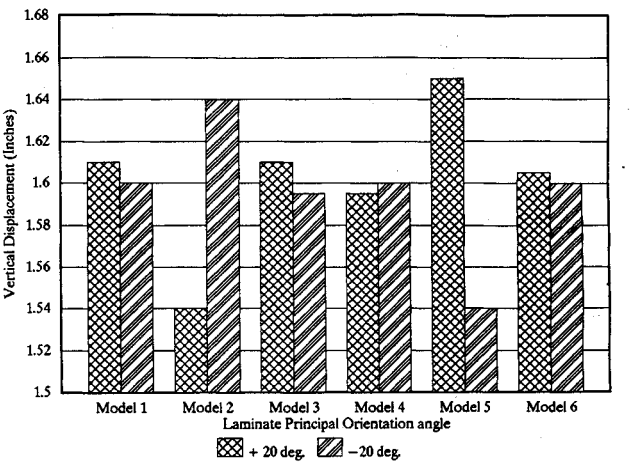

Fig. 4 Displacement at the tip due to vertical loads along the blade.

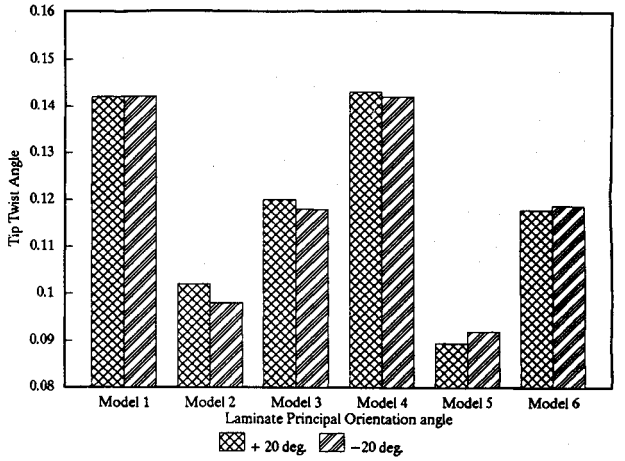

Fig. 3 Angular displacement at the tip due to pure torque.

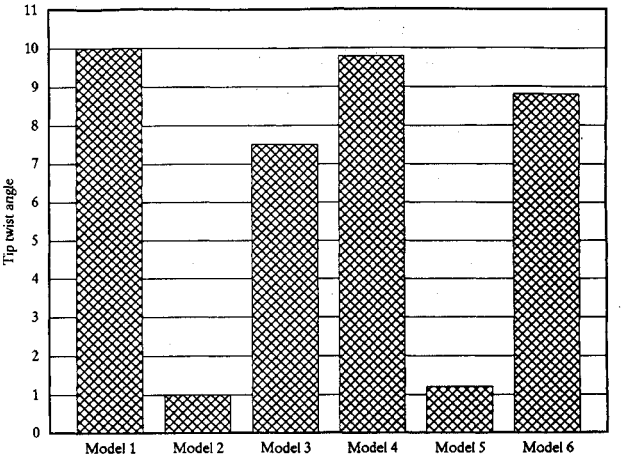

Fig. 5 Overall range of the available twist for the six models.

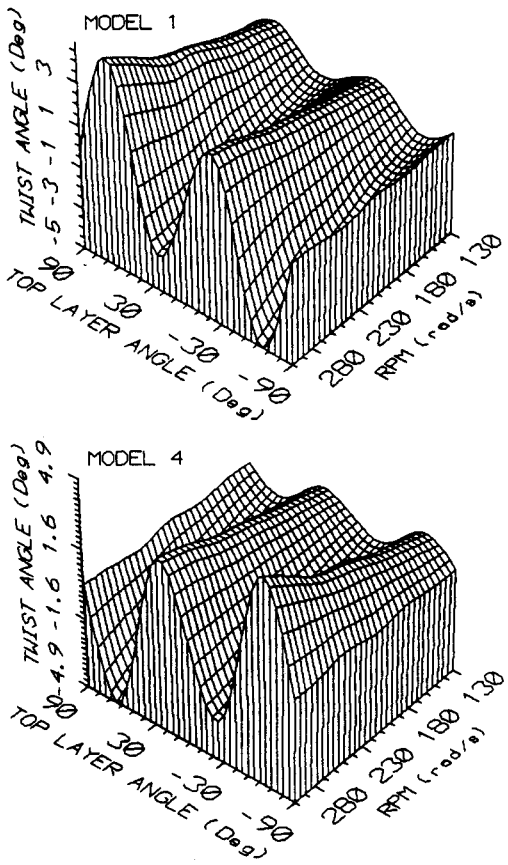

Fig. 6 Comparison of static behavior for models 1 and 4; inputs are rpm and LPO angle and response is the tip twist angle.

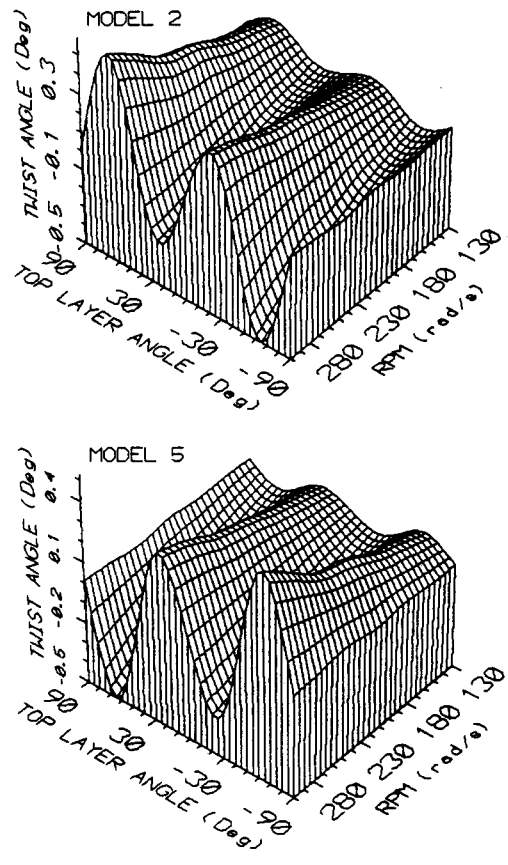

Fig. 7 Comparison of static behavior for models 2 and 5; inputs are rpm and LPO angle and response is the tip twist angle.

Torsional Load

A moment of 26.4 in./lb was applied, distributed among the nodes at the tip as concentrated moments. This load case revealed the influence of the LPO angle and the torsional stiffness for each model. The response of the six different models is presented for comparison purposes. The results are presented in Fig. 3 for the six models for LPOs of + 20 and −20 deg in each model. As much as 40% variation in the response may be observed in the comparisons.

Lift and Blade Weight Loads

This loading was designed to get the combined effect of the lift and blade weight reported in Ref. 5, and was expressed in terms of radial distance from the center as follows:

$$l = 0.02222\, r - 0.0123$$

where l is the load (lb/in.) varying as a linear function of the radial distance r.

The load was applied vertically along two spanwise rows at the leading and trailing edges, in a proportion that produced zero moments at the quarter chord. This load distribution was more homogeneous and induced less cross-sectional distortion, as opposed to the application along a line on upper surface as in beam-type elements. This distributed line loading produced small torsional displacement (of the order of 10^{-4} deg).

The results are presented in Fig. 4 for the six models, with two values of LPO (+20 and −20 deg) for each model.

Centrifugal Load

The next loading case investigated revealed the effect of varying centrifugal load, combined with changing the LPO angle within each model. The response yielded a twist angle induced by extension-twist coupling present in the structure due to asymmetric stacking sequence.

The loads due to lift and blade weight were present but their effects were observed to be negligible compared with those due to centrifugal loads.

The rpm was varied from 130 to 300 rad/s in increments of 10 rad/s, resulting in a total of 18 load cases. The combination of load cases and LPOs gave a total of 198 points of twist angle for each of the six models. These points are presented in six three-dimensional graphs to better appreciate the choices offered in this design approach. Those graphs present the trends of the twist angle with rpm and LPO variations. The twist angle range for each model is depicted in Fig. 5, while the overall parametric information is presented in Figs. 6–8.

Analysis of Results

This section presents the results obtained, keeping in view the two questions posed earlier. The responses under the loads mentioned for different configurations are presented.

The parameters considered are rpm and LPO as inputs and the twist-extension coupling manifested through the twist angle at the tip, as the output. This angle will be referred to as TTA (tip twist angle) in subsequent discussions.

The TTA can be used as a measure of the available twist for a given LPO (geometry and material system) and rpm. The twist angle for all load cases was found to be a nearly linear function of the radial distance.

From Fig. 2, it may be verified that models 1 and 4 can be built with only one unbroken piece of laminate, wrapped around a mold. Further, one model is just the inverse of the other, in other words model 1 is the inside-out of model 4. Models 2 and 5 can also be considered as some sort of inverse, in a broader sense; similar reasoning may be extended to models 3 and 6.

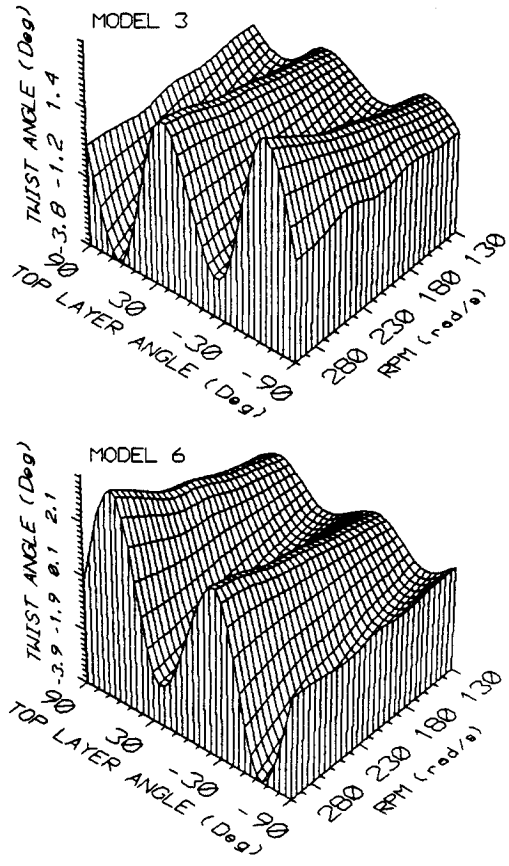

Fig. 8 Comparison of static behavior for models 3 and 6; inputs are rpm and LPO angle and response is the tip twist angle.

With the above considerations, the six models can be analyzed in pairs, which is very convenient from the point of view of getting the information in a simple and concise form, so that the designer can quickly evaluate a given model, keeping in view the design requirements.

The second important consequence of this inverse concept is that, models 1 and 4 can supply a spectrum of twist angle requirements for a given loading condition.

The importance of this resides in the manufacturing process, in that both models may be built by filament wound technique. This process is less expensive and more reliable, as it eliminates the filament discontinuity in the shell's junction and requires less accurate quality control.

The convention used in the modeling process has a side effect: namely, positive angles have an active aerodynamic stabilizing effect, acting as a propeller governor device.

1. Models 1 and 4—The response characteristics of the models, which were inverse to each other, are shown in Fig. 5 and behave as expected. This may be noted by observing the displacement for a given rpm and LPO angle as in Fig. 6.

2. Models 2 and 5—These models have the same inverse relationship in the TTA value. The main difference is that these two models are stiffer than the other four, as shown in Fig. 5. Figure 7 shows the response of the two models drawn together for different rpms and LPOs.

3. Models 3 and 6—The inverse relationship also holds here and the stiffness values are higher than that found in models 1 and 4 and lower than models 2 and 5 (Fig. 5). Figure 8 shows detailed comparisons for these two models.

These carpet plots may be constructed for other material systems by changing the orthotropic properties of the lamina, and thickness of lamina is yet another parameter that could be varied. Such plots are useful in the rotor blade design tradeoff studies.

Conclusions

This article presents a detailed analysis of a typical rotor blade, the focus being the static behavior in the presence of extension-twist coupling due to asymmetric stacking sequence of laminas. Different extension-twist coupling effects were obtained, by changing the ply orientation with respect to the body axes, for a chosen stacking sequence, thickness, and internal lay-up sequence. Also, a novel method is proposed to derive six configurations of a rotor blade system starting from a base rotor blade made of three laminated shells.

These effects are presented in terms of carpet plots. The extension-twist coupling is measured through the angular displacement at the tip of the blade as a function of rpm and LPO angle variations.

In the free vibration analysis performed for two LPOs for the six different models,[9] the first four fundamental frequencies vary very little for the six models considered.

The static analysis revealed a sort of "antisymmetric" behavior within the models, allowing them to be grouped in pairs. Such behavior can be of use in the design process, to trim structural response to prescribed loads.

Finally, care must be exercised in analyzing laminated composite structures. It is important to know how the local coordinate systems are established in the finite element program being used. These axes will determine the relative position of the laminate with respect to the structure. If asymmetries are present, it is possible to get different structural response for the same laminated composite rotor blades depending on the definition of the outward normal vectors of the surfaces that make up the blade.

Scope for Future Research

Future research may be beneficial in two areas. First, it is important to validate these models with experimental data, providing the necessary confidence in the modeling. Another field that calls for attention is the dynamic characteristics mapping, that is, with the rpm and LPO as parameters to obtain the fundamental frequencies as output. This would be an extension of Yntema's[10] work on beams of isotropic material to composite rotor beams.

Acknowledgments

The computer time was provided by the CAD/CAE Lab of the Department of Aeronautics and Astronautics.

References

[1]McVeigh, A. M., Rosenstein, H. J., and McHugh, F. J., "Aerodynamic Design of the XV-15 Advanced Composite Tilt Rotor Blade," *Proceedings of the 39th American Helicopter Society Annual Forum*, St. Louis, MO, May 1983, pp. 72–80.

[2]Nixon, M. W., "Extension-Twist Coupling of Composite Circular Tubes Applied to Tilt Rotor Blade Design," AIAA Paper 87-0733, Monterey, CA, April 1987.

[3]Lake, R. C., and Nixon, M. W., "A Preliminary Investigation of Finite Element Modeling for Composite Rotor Blades," NASA TM-100559, 1988.

[4]Computer Aided Structural Analysis/Graphical Interactive Finite Element Total System, *Users Reference and Primer Manuals*, CASA/GIFTS, Inc., Tucson, AZ, 1987.

[5]Hodges, R. V., Nixon, M. W., and Rehfield, L. W., "Comparison of Composite Rotor Blade Models: A Coupled-Beam Analysis and a MSC/NASTRAN Finite Element Model," NASA TM-89024, 1987.

[6]Rehfield, R. W., "Design Analysis Methodology for Composite Rotor Blades," *Seventh DoD/NASA Conference on Fibrous Composites in Structural Design*, Denver, CO, June 1985.

[7]Batoz, J. L., Bathe, K. J., and Ho, L. W., "A Study of Three-Node Triangular Plate Bending Elements," *International Journal for Numerical Methods in Engineering*, Vol. 15, 1980, pp. 1771–1812.

[8]Prouty, R. W., *Helicopter Performance, Stability and Control*, PWS Engineering, Boston, MA, 1986.

[9]Moura, G. A. M., "An Approach for Design and Analysis of Composite Rotor Blades," M.S. Thesis, Naval Postgraduate School, Monterey, CA, Sept. 1989.

[10]Yntema, R. T., "Simplified Procedures and Charts for the Rapid Estimation of Bending Frequencies of Rotating Beams," NACA TN-3459, 1955.